we did not identify the organisms in our samples, we believe that it is unlikely that species differences are responsible for the pattern we observed. Practically pure diatom samples collected in upwelling areas off Baja California (water temperature, 14.3°C) had Cd concentrations of up to 16.5 ppm, while in 23 diatom samples from Monterey Bay (temperature, 9.8° to 15.7°C) the highest Cd concentration was 4.8 ppm. One pure copepod sample from Baja California had a Cd concentration of 15.2 ppm, while the maximum was 6.0 ppm for ten Monterey Bay copepod samples. Many of the samples which had high Cd levels also contained high Sr concentrations. Samples with Sr-concentrating organisms from other areas were collected with the same fine-meshed nets; the Cd concentration was less than 2.2 ppm in four such samples collected 100 to 400 km northeast of Hawaii, less than 1.1 ppm in two samples collected off Oregon, and 3.4 ppm in a sample collected off Puerto Rico. Disregarding the zooplankton data and considering only the 89 samples collected with phytoplankton nets from inshore and offshore, tropical and temperate waters, we have never observed a Cd concentration greater than 7.5 ppm in any sample except those from the area south of San Diego off Baja California.

We believe that the increased Cd concentrations found south of San Diego are due to elevated concentrations in the water. Various hypotheses can be presented that could explain why Cd levels would be high in this area for both natural (*7*) and anthropogenic (*8*) reasons. However, until measurements of Cd in the waters off Baja California are made, further speculation is unwarranted. Nevertheless, the plankton data do suggest that an extraordinary situation in regard to this toxic element may well exist off Baja California. The reasons for its occurrence should be investigated.

J. H. MARTIN
W.W. BROENKOW
Moss Landing Marine Laboratories, Post Office Box 223, Moss Landing, California 95039

References and Notes

1. J. H. Martin and G. A. Knauer, *Geochim. Cosmochim. Acta* **37**, 1639 (1973); G. A. Knauer and J. H. Martin, *Limnol. Oceanogr.* **18**, 597 (1973).
2. R. R. Nilsson, *Aspects on the Toxicity of Cadmium and Its Compounds* (Swedish Natural Science Research Council, Stockholm, 1970), pp. 19–49.
3. Top predators such as sea lions (*Zalophus californianus*) and sea otters (*Enhydra lutris*) have renal Cd concentrations of up to 570 and 960 μg/g, dry weight, respectively (J. H. Martin, unpublished data).
4. Concentrations higher than the 3.5 and 3.9 ppm found north and south of Los Angeles could be expected because of the proximity of sewer outfalls from the city and county of Los Angeles. However, the samples were from depths of 0 to 5 m, and it is doubtful that these waters had mixed with Los Angeles waste waters since the outfall diffusers are at depths of 50 to 60 m and the effluent rises and spreads out along the thermocline, which was at 20 m when we sampled.
5. Several investigators measured Cd in Atlantic and Caribbean zooplankton during the International Decade of Ocean Exploration (IDOE) baseline studies (unpublished); almost all Cd concentrations in 248 samples were well below 10 ppm ("Baseline studies of pollutants in the marine environment," background papers for a workshop sponsored by the National Science Foundation's Office for the IDOE and held at Brookhaven, Upton, New York, 24 to 26 May 1972).
6. All readings were corrected for light scatter; see C. K. Billings, *At. Absorp. Newslett.* **4**, 357 (1965); K. Fletcher, *Econ. Geol.* **65**, 588 (1970). For further analytical details, see references in (*1*).
7. In waters like those off Baja California, upwelling currents may oppose the downward transport of organic material, and trace metal concentrations may become elevated in the surface waters because of the lack of biological removal. [D. F. Schutz and K. K. Turekian, *Geochim. Cosmochim. Acta* **29**, 259 (1965); J. P. Riley and D. Taylor, *Deep-Sea Res.* **19**, 307 (1972)].
8. Approximately 50 metric tons of Cd are introduced into the Southern California Bight annually via major submarine discharges of municipal waste water [*The Ecology of the Southern California Bight: Implications for Water Quality Management* (Southern California Coastal Water Research Project, El Segundo, 1973)]. However, provided adequate mixing occurs with California Current water, the 50 tons of Cd should be diluted to background levels long before reaching Baja California.
9. This research was supported by EPA grant R 802 350 and NSF grant GA 28306. We thank K. Baxter and G. Lopez for the R.V. *Alpha Helix* plankton samples; Oregon State University for the use of the R.V. *Cayuse*; and R. Flegal, K. Skaug, and P. Elliott for their help with the analyses and collections.

10 March 1975; revised 9 May 1975

Wurtzite: Long-Period Polytypes in Disordered 2H Crystals

Abstract. *An electron optical study of a disordered 2H wurtzite from Pribram, Czechoslovakia, reveals an even and dense distribution of stacking faults and indicates the presence of long-period polytypes. The polytype crystal structures appear quite distinct from those of synthetic equivalents, and this difference may be attributable to different environments of formation.*

Polytypic and disordered ZnS stacking sequences are transitional structural states between 2H wurtzite and sphalerite (*1*). In an electron optical investigation of a disordered natural 2H wurtzite, stacking faults, which mark departures from the ideal stacking sequence, are visible in bright- and dark-field modes. In addition, there is evidence of long-period polytypes which may represent a new family of polytypic structures. Their structures are apparently based on modulations of the 2H unit and thus are quite different from those of synthetic vapor-grown wurtzite polytypes (*2*). This difference may be a consequence of different environments of crystallization and, in addition, may reflect a different mode of polytype formation.

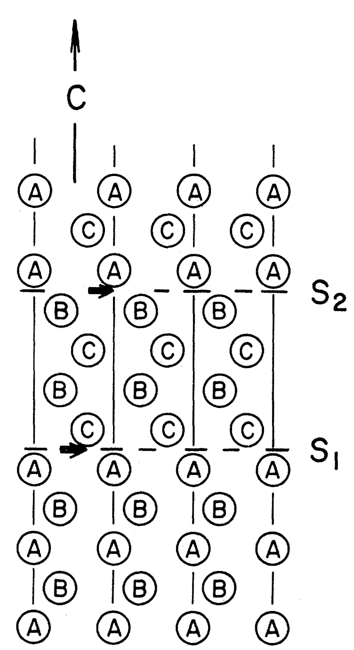

Fig. 1. Representation of a (110) layer three unit cells wide of a 2H wurtzite disordered by stacking faults: *A*, *B*, and *C* are either sulfur or zinc atoms; S_1 and S_2 are stacking fault planes; arrows are displacement vectors.

In 2H wurtzite and related structures all atoms lie on (110) planes (Fig. 1). Mistakes in the ideal stacking sequence can arise either during or after crystal growth because for each layer of atoms there are two nonequivalent atom positions which give identical nearest-neighbor environments. The mistakes (or stacking faults) occur as displacements of the atoms from their ideal positions by amounts of $\frac{2}{3} d_{100}$ [where d_{100} is the (100) interplanar spacing] and thus do not affect the intensity of diffracted x-ray and electron beams for which $h + k = 3n$, where n is an integer. However, on other reciprocal lattice rows random stacking faults produce diffraction streaks (*3*) and ordered stacking faults produce the diffraction maxima characteristic of a polytype.

The wurtzite studied, from Pribram, Czechoslovakia, is in the form of radiating aggregates of {001} plates. The average composition (in percentages by weight) as determined by electron microprobe analysis is as follows: zinc, 64.1; iron, 1.3; cadmium, 1.4; copper, 0.04; manganese, 0.01; and sulfur, 33.2. On single crystal x-ray diffraction precession films (*4*) reflections with $h + k \neq 3n$ are diffuse and elongated as apparently almost continuous streaks parallel to c^*, thus suggesting a very high degree of stacking disorder.

Electron optical observations were made with an electron microscope (AEI EM6G) at 100 kv on crushed grains. A typical zero level $h0\ell$ selected area diffraction pattern is

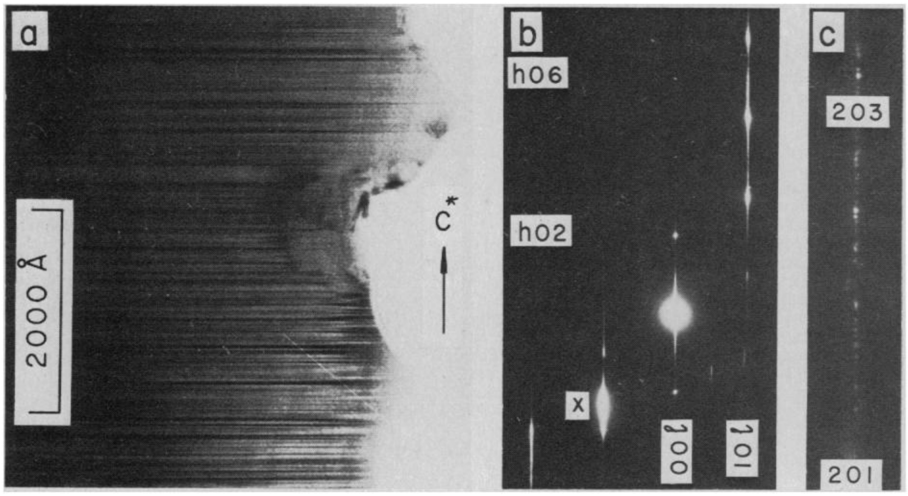

Fig. 2. (a) Bright-field micrograph of stacking faults in Pribram wurtzite. (b) Diffraction pattern of an area similar to that shown in (a); x is a diffuse maximum not related to a 2H reciprocal lattice point. (c) Enlargement of part of a 20ℓ row of another diffraction pattern showing diffraction maxima characteristic of a long-period polytype.

shown in Fig. 2b: such diffraction patterns are invariably eccentric since wurtzite does not cleave very readily on $\{110\}$. The reciprocal lattice rows with $h + k \neq 3n$ (10ℓ, 20ℓ, and so on) show continuous streaks, with diffuse maxima about 2H lattice points with $\ell = 2n + 1$, apparently consistent with the presence of random stacking faults. Other diffuse maxima on these rows (for example, x in Fig. 2b) are due to maximum diffraction contrast since they are displaced as the grains are tilted and correspond with bend contours in dark-field images. Bright-field images of grains parallel and subparallel to the a^*,c plane are crowded with diffraction fringes (Fig. 2a) which are normal to the diffraction streaks. One may image these fringes in dark field, using the diffraction streaks on reciprocal lattice rows with $h + k \neq 3n$ but not with reflections on other rows and they branch at thickness contours (*5*). Thus the fringes are clearly associated with stacking faults in the basal planes (*6*). The smallest fringe spacing observed is 20 Å, approximately equal to a 6H period, but the structural interpretation of this correlation may not be direct. The stacking fault density is particularly high, at least comparable to that of the so-called microtwins in inverted ZnS films (*7*), and its distribution is relatively even. The stacking faults are not terminated by partial dislocations, forming stacking faults in prism planes (*6*) or some other type of structural discontinuity, but appear to be continuous across the grains. Continuity is even maintained across embayments in crenulate grain boundaries, a clear indication that the stacking faults predate sample preparation.

On more detailed examination (Fig. 2c) the continuous diffraction streaks are sometimes seen to contain closely spaced diffraction maxima, the resolution of which varies markedly both between areas of a single diffraction pattern and between different diffraction patterns. Measurements on the diffraction pattern illustrated (Fig. 2c) indicate a periodicity relative to a 1H layer of 65, and measurements on five other patterns, all from different grains, give approximate periodicities of 100, 105, 130, 130, and 130, respectively. However, the accuracy of these latter data may be suspect because of poor contrast and limited continuity. It was clearly impossible to discriminate between hexagonal and rhombohedral patterns.

An obvious explanation for these diffraction maxima is that they represent ordered regions within a generally disordered 2H wurtzite matrix (*4*), each ordered region being a long-period wurtzite polytype directly analogous to the 594R polytype of SiC (*8*). The fact that the spacing and shape of the diffraction maxima do vary somewhat (Fig. 2c) may be attributed to one, or a combination of several, of the following factors: (i) long unit cells compared to the selected area aperture diameter and specimen thickness, (ii) incomplete long-range order, (iii) imperfect long-range order, and (iv) coherent scattering between the polytypic regions and the 2H wurtzite matrix. Theoretically, stacking faults are expected to be visible in both long-period polytypes and 2H wurtzite matrix, and these structurally distinct regions have not yet been resolved in bright- and dark-field electron optical modes. However, the apparently even and dense distribution of stacking faults in ordered regions coupled with the observation that the long-period diffraction maxima are superimposed on the 2H wurtzite pattern do suggest that structures of the Pribram polytypes are based on modulations of the 2H structural unit. These structures are quite unlike those of synthetic long-period polytypes, and this difference may be related to different thermal histories. The synthetic polytypes appear to develop during cooling after high-temperature crystal synthesis (*9*), whereas the Pribram wurtzite formed in a cavity in carbonate rock under geologically low-temperature conditions.

M. E. FLEET

Department of Geology,
University of Western Ontario,
London, Ontario, Canada

References and Notes

1. The crystal structure of 2H wurtzite may be represented by the stacking sequence ABABABA . . . and that of sphalerite by ABCABCAB . . ., where A, B, and C each represent a single stacking unit; H indicates hexagonal symmetry and R (below) rhombohedral symmetry.
2. I. T. Steinberger, I. Kiflawi, Z. H. Kalman, S. Mardix, *Phil. Mag.* **27**, 159 (1973).
3. A. J. C. Wilson, *X-Ray Optics* (Methuen, London, ed. 2, 1962), pp. 79–86.
4. M. E. Fleet, in preparation.
5. P. B. Hirsch *et al.*, *Electron Microscopy of Thin Crystals* (Butterworth, London, 1965), pp. 229–234.
6. H. Blank, P. Dealvignette, R. Gevers, S. Amelinckx, *Phys. Status Solidi* **7**, 747 (1964).
7. K. N. Rai, O. N. Srivastava, P. Krishna, *Phil. Mag.* **21**, 1247 (1970).
8. G. Honjo, S. Miyake, T. Tomita, *Acta Crystallogr.* **3**, 396 (1950).
9. E. Alexander, Z. H. Kalman, S. Mardix, I. T. Steinberger, *Phil. Mag.* **21**, 1237 (1970).
10. This study was carried out during sabbatical leave at the Department of Mineralogy and Petrology, University of Cambridge, with the use of facilities made available by Prof. W. A. Deer. I thank S. O. Agrell for providing the mineral specimen and J. D. C. McConnell and J. V. P. Long for technical assistance. Study supported by a National Research Council of Canada operating grant.

12 May 1975; revised 20 August 1975

Evolution of Type C Viral Genes: Origin of Feline Leukemia Virus

Abstract. *Reiterated gene sequences related to the RNA of feline leukemia virus (FeLV) are detected in all tissues of domestic cats and their close* Felis *relatives but not in more distantly related* Felis *species. Partially homologous viral gene sequences are found in rodent, and particularly rat, DNA. Together with the immunologic relationships observed between FeLV and endogenous rodent type C viruses, the results lead to the conclusion that FeLV-related genes were transmitted from a rodent to cat ancestor and have been perpetuated in the germ line of cats.*

Feline leukemia virus (FeLV) produces acute leukemia and lymphoma in domestic cats (*1*) and can be transmitted horizontally from animal to animal as an infectious disease (*2*). However, sequences partially related to the RNA genome of FeLV are